

Maize Early endosperm growth and development: From Fertilization through cell type differentiation¹

Brian M. Leroux², Austin J. Goodyke², Katelyn I. Schumacher², Chelsi P. Abbott², Amy M. Clore³, Ramin Yadegari⁴, Brian A. Larkins^{4,6}, and Joanne M. Dannenhoffer^{2,5}

²Department of Biology, Central Michigan University, Mount Pleasant, Michigan 48859 USA; ³Division of Natural Sciences, New College of Florida, Sarasota, Florida 34243 USA; and ⁴School of Plant Sciences, University of Arizona, Tucson, Arizona 85721 USA

- Premise of the study: Given the worldwide economic importance of maize endosperm, it is surprising that its development is
 not the most comprehensively studied of the cereals. We present detailed morphometric and cytological descriptions of endosperm development in the maize inbred line B73, for which the genome has been sequenced, and compare its growth with four
 diverse Nested Association Mapping (NAM) founder lines.
- Methods: The first 12 d of B73 endosperm development were described using semithin sections of plastic-embedded kernels and confocal microscopy. Longitudinal sections were used to compare endosperm length, thickness, and area.
- Key results: Morphometric comparison between Arizona- and Michigan-grown B73 showed a common pattern. Early endosperm development was divided into four stages: coenocytic, cellularization through alveolation, cellularization through partitioning, and differentiation. We observed tightly synchronous nuclear divisions in the coenocyte, elucidated that the onset of cellularization was coincident with endosperm size, and identified a previously undefined cell type (basal intermediate zone, BIZ). NAM founders with small mature kernels had larger endosperms (0–6 d after pollination) than lines with large mature kernels.
- Conclusions: Our B73-specific model of early endosperm growth links developmental events to relative endosperm size, while
 accounting for diverse growing conditions. Maize endosperm cellularizes through alveolation, then random partitioning of the
 central vacuole. This unique cellularization feature of maize contrasts with the smaller endosperms of Arabidopsis, barley, and
 rice that strictly cellularize through repeated alveolation. NAM analysis revealed differences in endosperm size during early
 development, which potentially relates to differences in timing of cellularization across diverse lines of maize.

Key words: alveolation; B73 maize; BETL; cellularization; cereals; coenocyte; differentiation; NAM; nuclear endosperm; Poaceae.

The development of endosperm is not only a defining synapomorphy of flowering plants, it also produces the seed component of cereal grains that supplies much of the world's food. The two products of double fertilization, the zygote and primary endosperm nucleus, develop through separate pathways. The endosperm, most commonly triploid in angiosperms (Brown and Lemmon, 2007; Williams and Friedman, 2002), is fated to become a nutrient-rich storage tissue that supports the growth of the diploid embryo. Two major model systems, the monocot cereals and the eudicot, *Arabidopsis*, undergo free nuclear endosperm development, which evolved independently in the monocots and multiple times in the eudicots (Floyd and Friedman, 2000). Endosperm development in cereals and *Arabidopsis* has routinely been described as involving three main

¹Manuscript received 26 February 2014; revision accepted 8 July 2014. The authors thank B. Hunter, J. Laurie, M. Skaggs, and D. Wang for assisting J.M.D. with collecting Arizona plant material. They thank B. Dilkes, G. Drews, and J. Gustin for insightful discussions. This research was supported by National Science Foundation grant IOS-0923880 (to A.M.C., R.Y., B.A.L., and J.M.D.). Additional support to J.M.D. was provided by a sabbatical leave from Central Michigan University.

⁵Author for correspondence (e-mail: danne1jm@cmich.edu)

⁶Present address: 230J Whittier Research Center, University of Nebraska, Lincoln, Nebraska, 68583 USA

doi:10.3732/ajb.1400083

cytological stages: coenocyte, cellularization by alveolation, and differentiation. The timing and pattern of these processes is different between the Arabidopsis and cereal model systems. Reviews of cereal endosperm development (e.g., Olsen et al., 1999; Olsen, 2001, 2004; Brown and Lemmon, 2007; Sabelli and Larkins, 2009; Becraft and Gutierrez-Marcos, 2012; Olsen and Becraft, 2013) often depict generalized developmental models that are largely based on comprehensive accounts of nuclei proliferation, microtubular networks, and phragmoplast or wall deposition in barley, rice, and wheat, with comparison to analogous observations in Arabidopsis (e.g., Mares et al., 1975, 1977; Morrison and O'Brien, 1976; Fineran et al., 1982; Van Lammeren, 1988; Mansfield and Briarty, 1990; Bosnes et al., 1992; Brown et al., 1994, 1996a, b, 1997, 1999, 2003; Olsen et al., 1995; Sørensen et al., 2002). Though these models and descriptions are often extended to all cereals, detailed cytological accounts of the coenocyte and cellularization stages of endosperm development in maize are generally much older and more limited (Randolph, 1936; Kiesselbach, 1949; Monjardino et al., 2007). Therefore, there is a need for a comprehensive evaluation of maize early endosperm development to highlight possible differences between cereals, as well as emphasize diversity in the nuclear endosperm development pathway with *Arabidopsis* as a comparative model.

Following fertilization in cereals and *Arabidopsis*, division of the primary endosperm nucleus and subsequent divisions of daughter nuclei is uncoupled from cytokinesis, allowing free

nuclear proliferation and formation of a coenocyte. In cereal endosperm, starting near the embryo, nuclei repeatedly divide synchronously and evenly space themselves until the nuclei line the periphery of the central vacuole (Randolph, 1936; Bennett et al., 1975; Olsen, 2001). Unlike cereals, the first three divisions in Arabidopsis produce evenly spaced nuclei throughout the endosperm periphery (Brown et al., 1999, 2003; Sørensen et al., 2002), but after the fourth division, the 16 nuclei no longer divide synchronously, and the endosperm can be divided into three domains that develop differently: micropylar endosperm near the embryo, peripheral endosperm of the central chamber, and chalazal endosperm near the nucellar proliferating cells (Boisnard-Lorig et al., 2001; Brown et al., 2003). Nuclei continue to proliferate within the micropylar and peripheral endosperm, whereas free nuclei in the chalazal endosperm form nodules of individual nuclei and a multinucleate cyst. At the coenocytic stage in cereals, the only region that has been identified is a basal sector of transfer cell precursors (Doan et al., 1996; Costa et al., 2003; Drea et al., 2005; Gutierrez-Marcos et al., 2006).

Initiation of cellularization occurs more rapidly in the small Arabidopsis endosperm, where nuclei are fewer (~200) and more widely spaced than in cereals, which are typically larger with more nuclei (~100s-1000s) and spend a longer time in the coenocyte stage (Bennett et al., 1975; Walbot, 1994; Brown et al., 1999). Transition to a cellular endosperm occurs via alveolation in both systems, beginning with the formation of anticlinal walls separating peripheral free nuclei of the coenocyte (Bosnes et al., 1992; Brown et al., 1994, 1999; Monjardino et al., 2007). Interaction of opposing microtubules from adjacent nuclear cytoplasmic domains brings about formation of adventitious phragmoplasts, and cell walls begin to form at the edge of the endosperm and advance inward in association with the phragmoplasts (Brown et al., 1994; Olsen et al., 1995). Newly formed anticlinal walls encase each peripheral nucleus in a tube-like structure, an alveolus, with an open periclinal face toward the central vacuole. Nuclear divisions within alveoli lead to deposition of periclinal walls that divide the alveoli into a peripheral cell and new alveolus. Though both cereals and Arabidopsis initiate cellularization near the embryo, there is a more pronounced gradient of alveolar development in Arabidopsis, where the chalazal endosperm cyst remains coenocytic to seed maturation (Mansfield and Briarty, 1990; Brown et al., 1999, 2003). Cereal endosperms become fully cellular by continuation of alveolation until the central vacuole is filled with cells (Kiesselbach, 1949; Bosnes et al., 1992; Brown et al., 1994; Becraft, 2001; Olsen, 2001); however, a more random pattern of cellularization of the inner central vacuole has been noted in maize (Monjardino et al., 2007).

Following cellularization, regions of the endosperm in both cereals and *Arabidopsis* differentiate into specialized cell types. The first cycle of cell division is formative in cereals, as the initial peripheral cell layer is fated to become aleurone. At seed maturation, the aleurone contains the only living cells of the endosperm, which are responsible for assisting in metabolite mobilization and germination (Becraft, 2001; Brown and Lemmon, 2007). The initial cells formed from the first division in *Arabidopsis* do not form a surrounding layer, but these cells persist until seed maturation and may perform aleurone-like functions (Brown et al., 1999). The chalazal region of *Arabidopsis* endosperm that remains a coenocytic cyst throughout development may perform a nutrient transfer function similar to the transfer cells found

in cereal endosperm (Brown et al., 1999). Central starchy endosperm cells accumulate storage products in both systems; these nutrients are used by the growing embryo before seed maturation in *Arabidopsis*, whereas in cereals these cells persist to kernel maturity. There are additional endosperm cell types found in cereals that are not observed in *Arabidopsis*, and likewise there is diversity in the number and complexity of these cell types among specific cereals (Olsen and Becraft, 2013). Given the large size of the maize grain, it is not surprising that maize has a larger endosperm with more cytologically identifiable cell types than smaller grain cereals, such as barley, wheat, and rice.

The worldwide economic importance of maize endosperm and the high degree of genetic and phenotypic diversity within maize germplasm (Liu et al., 2003; Flint-Garcia et al., 2005; Buckler et al., 2006) have made it a key model organism. Given the simplicity of controlled genetic crossings with maize (due to the physical separation of male and female flowers) and the high productivity of seeds from a single pollinated ear, maize has become the most thoroughly researched genetic system among cereals (Strable and Scanlon, 2009). The recently described maize reference genome (inbred line B73; Schnable et al., 2009) and the nested association mapping (NAM) population composed of 5000 recombinant inbred lines derived from crosses of B73 with each of 25 founder inbred lines that capture much of the genetic diversity of maize (Yu et al., 2008; McMullen et al., 2009) is fostering dissection of complex genetic traits. Subpopulations represented by the NAM founders include temperate stiff stalk, temperate non-stiff stalk, tropical or semitropical, popcorn, and sweet corn (Liu et al., 2003), and manifest the diversity of ear and plant morphology (McMullen et al., 2009). These genetic materials are ideal for comparisons of endosperm development across the diversity of maize germplasm.

We undertook an in-depth analysis of maize endosperm growth and cytological development in B73, because of its importance as a model against which other maize lines will be compared. Previous research described early endosperm size at selected ages in "Pride of Michigan" (Randolph, 1936), a locally adapted yellow dent corn (Kiesselbach, 1949), A-188 (Schel et al., 1984), W23XM14 (Phillips and Evans, 2011), and W64A (Monjardino et al., 2007), but there are vast differences in these genotypes. When compared with B73, fellow founder line Mo17 has been shown to have hundreds of genes with copy differences, and almost 200 genes present in one line and not in the other (Springer et al., 2009). A detailed study of endosperm growth and development in B73 will allow comparison of gene expression and developmental and cytological events in other genotypes, including the NAM lines

Our objective was to methodically detail, through morphometric and cytological descriptions, B73 endosperm development and growth from fertilization to differentiated cell types. The goals were to (1) compare endosperm and kernel size in different growing conditions; (2) detail early development stages (coenocyte, cellularization, and differentiation) in concert with endosperm size; and (3) compare the results with selected NAM founder lines to ascertain diversity in endosperm size during early development. This work provides a framework to better understand how gene expression in B73 during early endosperm growth relates to the timing and structure of endosperm developmental events.

MATERIALS AND METHODS

Plant material—Zea mays L. inbred line B73 (PI 550473) was greenhousegrown in Arizona (AZ) under a 16 h photoperiod maintained using 1000 W high pressure sodium lamps. Plants were grown in 11-L pots, fertilized with Peters 20:20:20 NPK (Scotts Co., Marysville, Ohio, USA) and supplemented with Ca(NO₃)₂, KNO₃, and chelated iron at each watering. B73 was field-grown in Michigan (MI), where plants were provided supplemental water and fertilized with Schulz 20:20:20 NPK (Infinity Fertilizers, Rock Island, Illinois, USA) approximately biweekly. Plants at both locations were self-pollinated or, infrequently, pollinated by a sibling and harvested 0–12 d after pollination (DAP). Kernels were preferentially sampled from the central portion of ears, in areas of uniform seed set. For anatomical analysis, MI kernels were fixed and stored at 4°C in either 4% formaldehyde–1% glutaraldehyde in 100 mmol/L potassium phosphate buffer pH 6.8 or 2% formaldehyde–0.25% glutaraldehyde in 50 mmol/L potassium phosphate buffer pH 7.

To compare observations in B73 with patterns of endosperm growth across diverse maize lines, we chose two NAM founder representatives with large mature kernel size (Ky21 and M162W) and two with small mature kernel size (Hp301 and P39) based on kernel length and mass measures from the Maize Diversity Project phenotype database (http://www.panzea.org). In addition to genetic diversity and mature kernel size variation, these lines also represent a diversity of subpopulations including stiff stalk (B73), non-stiff stalk (Ky21 and M162W), sweet corn (P39), and popcorn (Hp301) (Liu et al., 2003). Inbreds Hp301 (PI 587131), P39 (Ames 28186), Ky21 (Ames 27130), and M162W (Ames 27134) were field-grown in MI and processed in the same manner as B73 material.

Comparative morphometrics—Stereomicroscopy and imaging—For compartment measurements of length, thickness, and area of AZ kernels medial longitudinal hand sections through the embryo of fresh kernels were stained with 0.05% (w/v) aqueous toluidine blue O (TBO), and micrographs were taken immediately using an Olympus SZX12 Zoom stereomicroscope (Olympus Imaging America, Center Valley, Pennsylvania, USA). For all lines grown in MI, fixed kernels were rinsed in phosphate-buffered saline (PBS) and sectioned at 150–200 μm with a Vibratome 1000 Plus Sectioning System (Ted Pella, Redding, California, USA). Medial longitudinal sections were stained in TBO, rinsed in PBS, and mounted in Fluoromount (Sigma-Aldrich, St. Louis, Missouri, USA) or 10% w/v polyvinyl alcohol (PVA)–2.5% w/v 1,4-diazabicy-clo[2.2.2]octane (DABCO) in 25 mmol/L Tris, pH 8.7. Micrographs were taken immediately with a Nikon SMZ-2T stereomicroscope using a Zeiss AxioCam MRc equipped with AxioVision 4.5 software (Carl Zeiss, Oberkochen, Germany).

<code>Measurements</code>—Micrographs were analyzed with Image-Pro Plus 4.0 software (MediaCybernetics, Rockville, Maryland, USA) to measure kernel compartments. Linear length and thickness measures were calculated through the largest point of each compartment using the line tool. Area measures were calculated using the polygon tool (free trace option), with the pedicel and silk excluded from kernel area measures. For each kernel compartment, internal structures were excluded; for example, endosperm area was traced to exclude the embryo. For B73 grown in AZ and MI, up to nine kernels (from a minimum of two plants) were measured at 0–12 DAP ($N_{\rm AZ}=65;N_{\rm MI}=84$). For comparisons across lines, up to nine kernels (from a minimum of two plants) were measured for 0–6 DAP ($N_{\rm B73}=57;N_{\rm Hp301}=57;N_{\rm Ky21}=57;N_{\rm P39}=57$ and $N_{\rm M162W}=53$).

Growing degree-days (GDD) calculation—To compare AZ- and MI-grown B73 endosperms and account for thermal differences in growing conditions (AZ greenhouse mean = 31°C day and 21°C night; MI field mean = 28°C day and 18°C night), we converted DAP to GDD. A mean daily GDD was calculated for each location as follows: $_{\rm GDD} = \frac{T_{\rm MAX} + T_{\rm MIN}}{T_{\rm MIN}} - T_{\rm MAX}$ was the mean daily high, $T_{\rm MIN}$ was the mean daily low, and $T_{\rm BASE}$ was, as previously described for maize (Cross and Zuber, 1972), set to 10°C.

Data analysis—Endosperm measures were compared using Minitab 16 (Minitab, State College, Pennsylvania, USA). Measures of endosperm area, length, and thickness were divided by area, length, and thickness measures for the kernel to generate equal variances within the samples, then log10-transformed to normalize the data. A 2-way MANOVA was used to compare B73 kernel-proportional endosperm area, length, and thickness across DAPs and between locations (AZ and MI). Kernel-proportional endosperm area among B73 and

other selected NAM founder lines was compared with a 2-way ANOVA. Differences in both cases were determined by conducting a posthoc Tukey multiple comparisons test with a 95% confidence interval. Discriminant analysis classification was used to determine whether DAP groups could be determined from kernel-proportional measures of B73 endosperm area, length, and thickness. This analysis was performed for AZ kernels, MI kernels, and then all kernels pooled.

Endosperm anatomy—Bright-field microscopy and imaging—Fixed kernels were processed for plastic embedment. Briefly, kernels were rinsed in a 50 mmol/L potassium phosphate buffer, postfixed in 2% (v/v) osmium tetroxide, and dehydrated in a graded ethanol series followed by infiltration with Spurr's resin (Spurr, 1969). Semithin sections (1–2 $\mu m)$ were cut using a RMC Powertome (Boeckler Instruments, Tucson, Arizona, USA), stained with TBO, visualized with a Zeiss AxioPhot microscope, and photographed with a Zeiss AxioCam MRc as above.

Confocal microscopy and imaging—For confocal microscopy (except for one sample; Fig. 3I, J), fixed kernels were rinsed in PBS and stained with 0.04% v/v propidium iodide in PBS for 5 min prior to vibratome sectioning at $\approx 125~\mu m$. Sections were incubated for 15 min at 37°C in 0.8% w/v cellulase in 0.4 mmol/L phenylmethylsulfonyl fluoride, rinsed with PBS then incubated for 30 min in 0.1% v/v Triton X-100 in PBS. Kernels were rinsed in PBS, stained in 0.1 mmol/L Sytox Green (Molecular Probes, Eugene, Oregon, USA) in dimethyl sulfoxide, and mounted in PVA/DABCO. Material was imaged using $10\times$ (NA = 0.4), $20\times$ (NA = 0.7), $40\times$ (NA = 0.75), and $60\times$ oil immersion (NA = 1.4) objectives on an Olympus Fluoview 300 confocal laser scanning microscope using argon (488 nm excitation) and green helium/neon (543 nm excitation) lasers.

One endosperm processed for nuclear localization using 4',6-diamidino-2-phenylindole dihydrochloride (DAPI) staining was fortuitously caught during telophase. The fixed kernel was dehydrated and embedded in Steedman's wax (Ruzin, 1999) before cutting 20 μm sections using a Spencer 820 rotary microtome (American Optical, Buffalo, New York, USA). Sections were dewaxed, rinsed in PBS buffer and stained for 10 min in 100 $\mu g/mL$ DAPI before being mounted in PVA/DABCO. The endosperm was imaged with a Nikon A1R confocal laser scanning microscope (Nikon Instruments, Melville, New York, USA) using 20× (NA = 0.75) and 60× oil immersion (NA = 1.4) objectives with the Ti sapphire diode (403 nm excitation). Autofluorescence from the glutaraldehyde-fixed tissue was visualized for contrast using a Coherent Cube (Santa Clara, California, USA) laser (560 nm excitation).

Endosperm nuclei counts and cell measurements—The number of nuclei in coenocytic endosperms was counted from serially sectioned, plastic-embedded endosperms, from 1-4 DAP in age. Overlays were positioned on successive images and individual nuclei identified and followed in series. Alveoli, cell, and compartment sizes during cellularization (4-6 DAP, MI material) and cell size (12 DAP, MI material) were measured from semithin plastic sections using Image-Pro Plus (Media Cybernetics, Rockville, Maryland, USA). Mean length of cells and alveoli during various stages of cellularization were measured with at least 40 measures taken from at least two plants for a total of N = 455. Measures were log-transformed for normality and compared with an ANOVA followed by a Tukey test to identify differences with a 95% confidence interval. For further distinguishing cell types, a total of 88 measures from four plants were taken from longitudinal and cross sections. In longitudinal sections, we measured length as the longest axis; in cross section, we measured diameter of the cell at two perpendicular axes and then pooled these measures for reporting. Differences between length measures were analyzed with an ANOVA followed by a Tukey multiple comparison test with a 95% confidence interval.

Figure manipulations—All micrographs were processed in Adobe Photoshop CS5 (Adobe Systems, San Jose, California, USA) and image adjustments, when used, were one-time applications to the entire image to amend brightness and contrast.

RESULTS

Morphometrics—The mean area occupied by each of the kernel compartments (pericarp, nucellus, endosperm, and embryo) over the first 12 DAP of B73 maize grown in MI and AZ showed

a similar pattern of compartment development (Fig. 1A, B). Over this developmental time, the nucellus decreased from about 50% of the kernel area to being completely depleted by 10 DAP in AZ kernels and by 12 DAP in MI kernels. In both locations, the embryo size was negligible; at 12 DAP, the embryo occupied only about 5% of the kernel area in AZ kernels and 2% in MI kernels.

The pattern of endosperm growth in AZ- and MI-grown plants was different ($F_{1,125} = 45.08$, P < 0.0001); kernels in AZ grew faster and larger. Endosperm area increased as a proportion of kernel size over the first 12 d of development ($F_{11.125}$ = 213.17, P < 0.0001). Although the endosperm was undergoing nuclear proliferation as a coenocyte during the first 3 DAPs, it did not increase in size from that of the unfertilized embryo sac, which was approximately 2% of the kernel area at this stage (Fig. 1A-C). In AZ, the endosperm increased rapidly in size after 3 DAP, becoming approximately 30% of the kernel by 8 DAP (Fig. 1A, C). Kernels grown in MI had a delay of 1-2 d before this rapid increase in endosperm size with a similar increase in growth at 4-5 DAP (Fig. 1B, C). By 8 DAP, the endosperm of MI-grown kernels accounted for only about 20% of the kernel area. In AZ, after an incremental size increase the endosperm area plateaued after 10 DAP, accounting for ~70% of the kernel. In MI, endosperm area was only slightly more than 60% of the kernel at 12 DAP and appeared to be decreasing in growth rate. When DAP was converted to GDD to account for environmental variation, the pattern of endosperm growth between the two locations was almost identical (Fig. 1D).

Similar to area, both endosperm length ($F_{11, 125} = 83.78, P <$ 0.0001; Fig. 1E) and thickness ($F_{11, 125} = 199.00$, P < 0.0001; Fig. 1F) increased as a proportion of the kernel over the first 12 d of development. Kernel-proportional length and thickness of the embryo sac was 20% and 10%, respectively, and after fertilization, the endosperm increased in size to more than 80% of the kernel by 12 DAP (Fig. 1E, F). Endosperm length ($F_{1.125}$ = 67.62, P < 0.0001) and thickness $(F_{1, 125} = 26.01, P < 0.0001)$ as a proportion of kernel size were larger in AZ compared with MI kernels. A discriminant analysis was able to correctly classify endosperm measurements into DAP as a function of endosperm area, length, and thickness relative to kernel size at a correct rate of 53.8% for AZ kernels, 61.9% for MI kernels, and 43.0% for kernels regardless of location. Mean endosperm area, length, and thickness in longitudinal section from AZ and MI kernels, as well as mean endosperm width in cross section from MI kernels, is presented in Appendix S1 (see Supplemental Data with the online version of this article).

Cytology—Endosperm development in B73 from a fertilized triploid nucleus to a fully cellular and differentiating tissue occurred in four cytologically identifiable stages: coenocytic, alveolation, partitioning, and differentiation (Fig. 2). This process was continuous with some variability and overlap in timing among kernels, but it corresponded with the pattern of endosperm size increase during the first 12 d of development (Fig. 1D). Cellularization began ~40–46 GDD (~2.5 and 4 DAP in AZ- and MI-grown kernels, respectively) and ended at ~65–72 GDD (~4 and 5 DAP in AZ- and MI-grown kernels, respectively). In the first stage following pollination, the coenocytic stage, the endosperm was developing but not growing in size. During the subsequent two stages, cellularization through alveolation and then through partitioning, the endosperm area increased and cellularization appeared to commence when the

endosperm had approximately doubled in size. The period of rapid exponential growth was when the endosperm was fully cellular and differentiating. Because the differences in endosperm size between AZ- and MI-grown kernels could be accounted for by environmental conditions, as shown by the GDD conversion, cytological staging of endosperm development was not classified based on DAP.

Coenocytic stage—Endosperms at the coenocytic stage had nuclear division without cytokinesis (Fig. 3), and the free nuclei shared a common cytoplasm around a central vacuole. As the nuclei divided mitotically, they lined the wall starting near the embryo and kernel base (Fig. 3A, G) and then migrated toward the antipodal end of the endosperm (Fig. 3B) until they were distributed along the wall of the entire endosperm (Fig. 3C, D, H, I). The endosperm contained cytoplasm without and with conspicuous vacuoles (compare Fig. 3E, F).

Endosperm area measurements and nuclei counts showed that smaller endosperms had few nuclei that were located at the bottom, whereas larger endosperms had many nuclei that were dispersed throughout (Table 1). Endosperms with nuclei positioned only at the base never contained more than 16 nuclei. Endosperms with nuclei distributed throughout contained as few as 64 nuclei.

The parietal nuclei were evenly spaced around the central vacuole (Fig. 3D) and were surrounded by cytoplasmic domains (Fig. 3K). Two endosperms were observed showing nuclei synchronously dividing; they were observed with all nuclei either in prophase (Fig. 3K) or telophase (Fig. 3I, J). An endosperm containing only 128 nuclei was found in which cellularization proceeded (Table 1), while another contained 512 free nuclei without evidence of cell wall formation (Fig. 3I, J).

Alveolation stage—The process of endosperm cellularization proceeded in two stages, the first being alveolus formation (Fig. 4). The first layer of alveoli was formed by anticlinal wall deposition around each parietal nucleus, perpendicular to the endosperm cell wall (Fig. 4A-E). The anticlinal walls extended toward the central vacuole and the surface adjacent to the central vacuole remained open. The first alveoli formed near the embryo and at the base of the endosperm. Some endosperms were observed with alveoli at the base and free nuclei at the tip (Fig. 4I). An individual alveolus contained one to a few nuclei (Fig. 4C–E, J), and those nuclei could be oriented anticlinally (Fig. 4C) or periclinally (Fig. 4J). When the first periclinal wall formed in an alveolus, a small peripheral cell formed at the outer edge of the endosperm leaving a secondary alveolus with anticlinal walls extending toward the central vacuole. Secondary alveoli were larger than primary alveoli, and the cells formed by them were larger than the initial peripheral layer of cells $(F_{5,449} = 74.75, P < 0.0001; Fig. 5)$. The process of cellularization through alveolation continued until 2-4 cell layers were formed (Fig. 4F–H, K).

Partitioning stage—Alveolation formed only 2–4 cell layers, and subsequent cellularization occurred by partitioning of the remaining central vacuole (Fig. 6). The partitions were formed when the last secondary alveoli had anticlinal walls that continued to extend toward the center of the endosperm until they contacted another anticlinal wall extending from a different location (Fig. 6A, B, E). The large partitions formed by the anticlinal walls meeting each other were longer than the primary alveoli; and they were subsequently subdivided into smaller

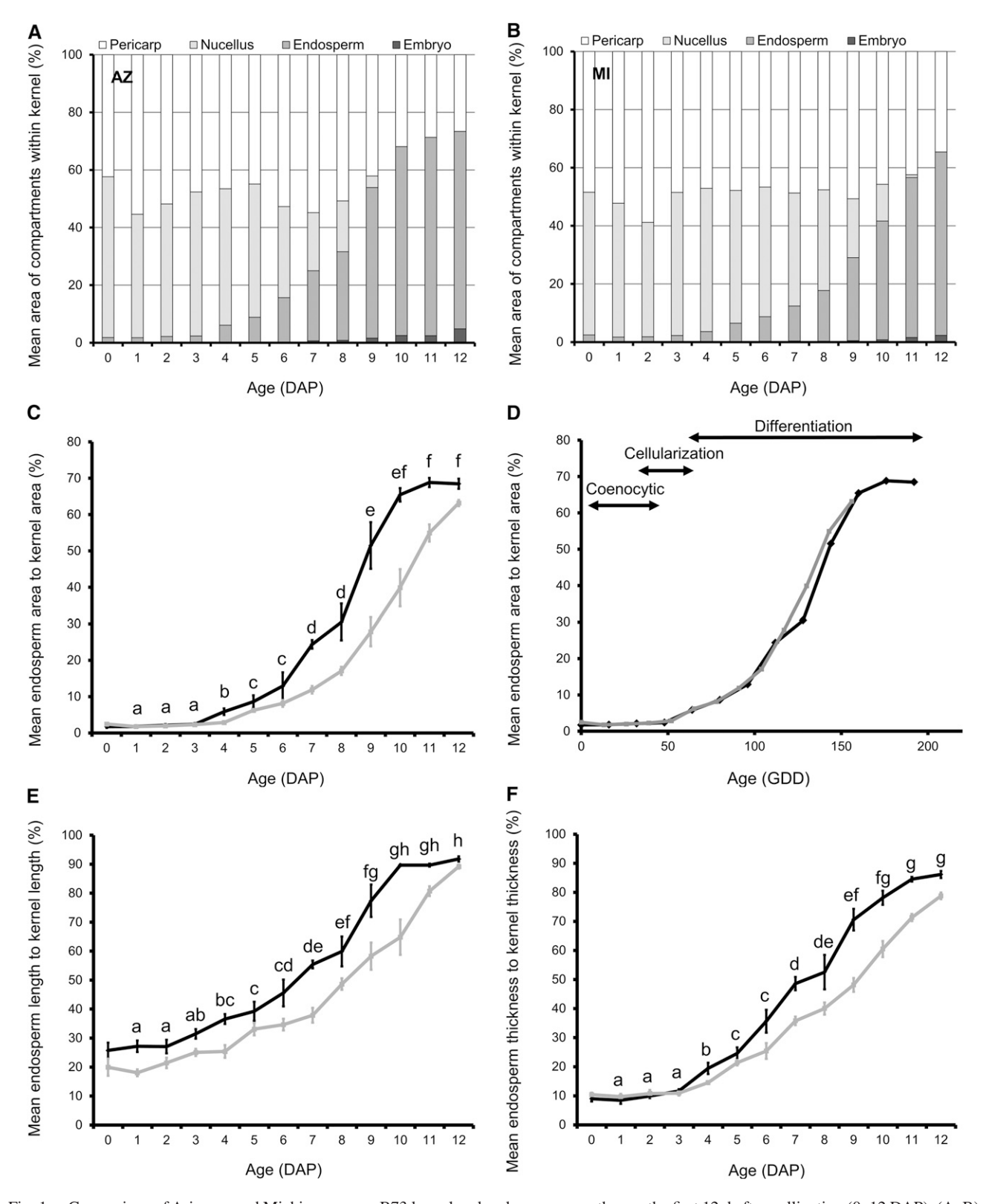


Fig. 1. Comparison of Arizona- and Michigan-grown B73 kernel and endosperm growth over the first 12 d after pollination (0-12 DAP). (A, B) Mean kernel compartment area as a percentage of kernel area for (A) AZ and (B) MI. (C-F) Comparison of mean endosperm sizes of AZ (black) and MI (gray) kernels. Bars indicate standard errors. Letters above the lines indicate where pooled (AZ and MI) ages were significantly different (P < 0.05). (C) The proportion of kernel area occupied by endosperm increased significantly after 3 DAP, with more rapid growth observed after 6 DAP. (D) The pattern of kernel area occupied by endosperm over development in AZ vs. MI is comparable when DAP is converted to growing degree-days (GDD). (E, F) Mean kernel-proportional endosperm (E) length and (F) thickness showed similar patterns to area, with endosperm length being the dimension that showed the greatest variability over early development.

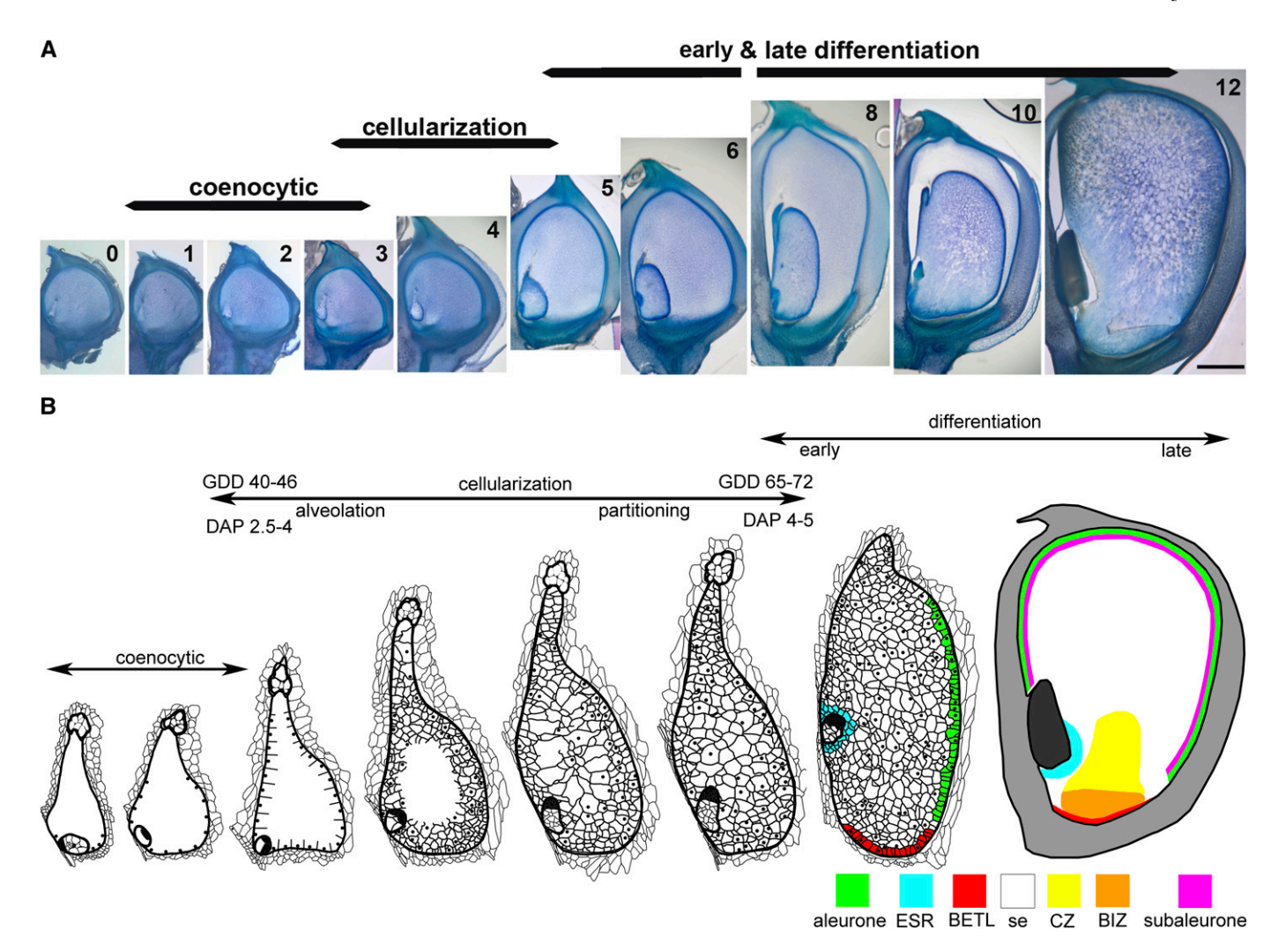


Fig. 2. Micrographs and model of B73 maize early endosperm development from a coenocyte to a differentiating endosperm before accumulation of storage metabolites. (A) Micrographs are of progressively older kernels (0–12 d after pollination [DAP]) longitudinally sectioned and stained with toluidine blue. (0) Kernel with unfertilized embryo sac. (1–3) Kernels similar in size with small coenocytic endosperm. (4) Enlargement of endosperm obvious with development of bulbous base. (5–6) Significantly larger and fully cellular endosperm by 5 DAP with identifiable embryo. (8–12) Later stages of cellular endosperm showing rapid growth and more than doubling of endosperm size in each successive image, or approximately every 2 d. All micrographs are presented with embryo to the left and endosperm base at same level. Bar = 1 mm. (B) A schematic highlighting major cytological transitions, timing of transitions, and location of differentiated cell types. *Abbreviations:* BETL, basal endosperm transfer layer; BIZ, basal intermediate zone; CZ, conducting zone; ESR, embryo surrounding region; GDD, growing degree days; SE, starchy endosperm.

cells in a less organized fashion (Figs. 5, 6F, 6G). During subdivision, some cells contained three nuclei (Fig. 6C, D).

Early differentiation—Following cellularization, the endosperm was differentiated into four cell types: the embryo surrounding region (ESR), immature starchy endosperm (SE), basal endosperm transfer layer (BETL), and aleurone (Fig. 7A). The ESR consisted of densely cytoplasmic cells with very small vacuoles. The ESR was initially evident surrounding the entire embryo, but later the ESR was most prominent around the suspensor portion of the embryo (Fig. 7B). At this time, ESR cells were isodiametric in shape and were among the smallest cells in

Fig. 3. Light and confocal micrographs of B73 maize endosperms during the coenocytic stage. Embryo (E) when present is to the left. (A–F) Plastic sections stained with toluidine blue. (A–C) Longitudinal sections of coenocytic endosperms. Arrowheads indicate most apical nucleus in each endosperm. (A) Four basal nuclei at micropylar end of endosperm. (B) Endosperm with more nuclei, which are starting to move up the sides. (C) Endosperm with nuclei throughout. (D) Cross section of coenocytic stage showing parietal nuclei throughout the endosperm. (E, F) Glancing sections showing parietal nuclei in common cytoplasm. (E) Cytoplasm without vacuole but apparent lipid. (F) Cytoplasm with vacuoles. (G–K) Confocal micrographs taken from tissue stained two ways: (G, H, K) single optical sections where cell walls and cytoplasm (red) were stained with propidium iodide (PI) and nuclei (yellow) double-stained with PI and SYTOX Green; (I, J) extended-focus confocal micrographs of glutaraldehyde-fixed autofluorescing tissue (red) and nuclei (blue) stained with DAPI. (G) Nuclei in basal location. (H) Evenly spaced nuclei at base of endosperm. (I) Low and (J) high magnification views of nuclei in telophase throughout the endosperm. (K) Nuclei in prophase with condensed chromosomes (yellow) surrounded by cytoplasmic domains. Bars = $100 \mu m$ (A–D, G–I) and $25 \mu m$ (E, F, J, K).

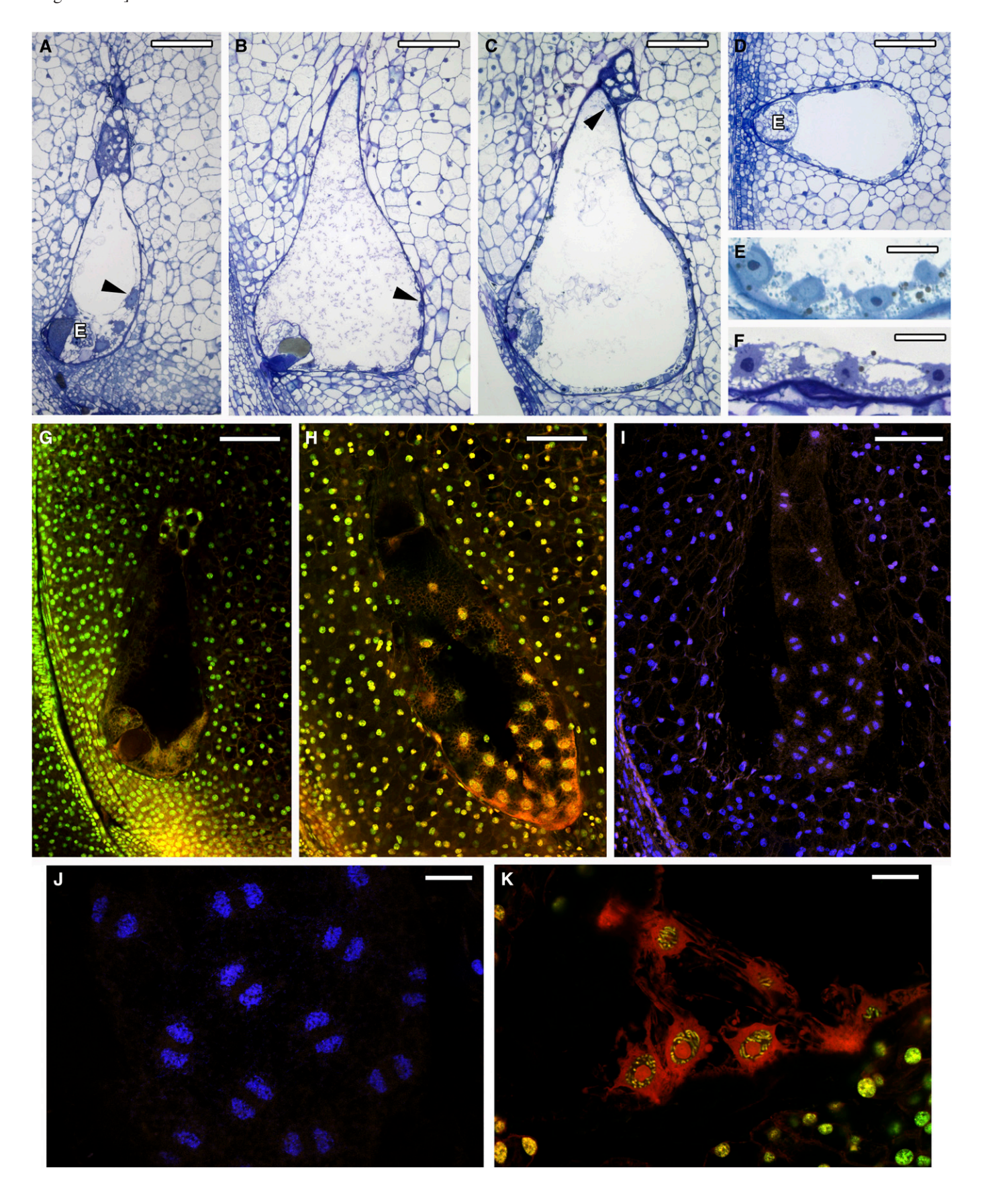


Table 1. Number of nuclei, location of nuclei, and endosperm size from serially sectioned B73 maize endosperms by developmental stage.

Stage	Endosperm area (mm²)	Nuclei number	Nuclei location
Coenocyte	0.037	8	Bottom
Coenocyte	0.054	16	Bottom
Coenocyte	0.061	16	Bottom
Coenocyte	0.053	16	Sides
Coenocyte	0.060	16	Sides
Coenocyte	0.084	16	Sides
Coenocyte	0.104	64	Throughout
Coenocyte	0.103	128	Throughout
Coenocyte	0.124	512 a	Throughout
Alveolation	0.161	128	C

^a Due to the preparation method of the tightly synchronous telophase endosperm (confocal optical-sectioning of 11 paraffin sections), the endosperm was incomplete, so we rounded the nuclei count up to 512.

the endosperm. Large, highly vacuolated immature SE cells occupied the central portion of the endosperm, and though not yet accumulating starch were occupying the space later to become the starchy endosperm (Fig. 7C). Cells constituting the BETL were located at the base of the developing endosperm, adjacent to the maternal placental-chalazal region; these cells were slightly elongate, had dense cytoplasm, and did not yet have the characteristic wall ingrowths (Fig. 7D). The remaining cells formed by the first round of alveolation at the edge of the endosperm differentiated into aleurone (Fig. 7E). These relatively small cells were cuboidal in shape and were developing multiple large conspicuous vacuoles.

Late differentiation—Later in development, the ESR, BETL, SE, and aleurone cells were further differentiated, and three additional cell types were observed: subaleurone, conducting zone (CZ), and a newly elucidated cell type we describe as the basal intermediate zone (BIZ) (Fig. 8). A distinct and recognizable ESR was almost exclusively limited to the suspensor portion of the embryo (Fig. 8A, B). It appeared that the developing embryo pushed away and crushed the ESR cells as it grew. The remaining ESR cells were slightly elongate and more highly vacuolated than before (compare Figs. 7B and 8A, 8B).

At the endosperm edge, aleurone, subaleurone, and SE cells were easily distinguishable and appeared similar to this area in kernels at later stages of starch and protein accumulation (Fig. 8C, D). Aleurone cells maintained their boxy shape, had dense cytoplasm with few small vacuoles, and accumulated lipids. The cell layer directly beneath the aleurone differentiated into the meristematic subaleurone. It was similar in shape and size to the aleurone and contained recent cell divisions that resulted in extension of the endosperm and formation of SE cells. The cytoplasm of these cells was more highly vacuolated and slightly less dense than that of an aleurone cell. The gradient in SE cell and nuclear size increased from the small cells next to the subaleurone to the larger inner SE cells that accumulated storage compounds.

The BETL (Fig. 8G, H) contained a single layer of cells that were visibly elongate, approximately two times longer than wide (long axis mean = $40.65~\mu m \pm 3.11$, cross axis mean = $22.29~\mu m \pm 1.01$), with prominent and extensive wall ingrowths. The cells had dense cytoplasm and contained many vacuoles. Some vacuoles were small, but others were very large, sometimes occupying nearly half the cell volume.

The CZ (Fig. 8E, F) contained large cells that were extremely elongate, approximately 3.5 times longer than wide (long axis

mean = $279.02 \, \mu m \pm 14.16$, cross axis mean = $78.98 \, \mu m \pm 2.61$), with tapering end walls. Cells in the CZ had sparse cytoplasm, no distinct vacuoles and very large, prominent nuclei. The CZ cell walls had no ingrowths; however, their longitudinal walls at times appeared to be rippled.

In the central basal portion of the kernel, the CZ cells were separated from the BETL by cells of intermediate size, content, and wall characteristics that we term the basal intermediate zone (BIZ; Fig. 8G, H). Cells constituting the BIZ near the BETL had smaller and less-developed wall ingrowths than the adjacent BETL, but BIZ cells near the CZ had no wall ingrowths like the adjacent CZ. Cells constituting the BIZ near the BETL had many small vacuoles, some large vacuoles, and a moderately dense cytoplasm surrounding these vacuoles. Near the CZ, the BIZ cells displayed decreasingly dense cytoplasm and fewer vacuoles. Nuclei in the BIZ appeared slightly larger than the BETL nuclei, but much smaller than the nuclei in the CZ. Cells in the BIZ were approximately 2.5 times longer than wide (long axis mean = $103.68 \mu m \pm 9.51$, cross axis mean = 37.83 $\mu m \pm 1.30$) and were intermediate in size compared to BETL and CZ cells. There were significant differences between BETL, CZ, and BIZ cell measurements in long-axis length $(F_{2,20} = 88.53, P < 0.0001; Tukey P < 0.05).$

NAM founder analysis—The NAM founder inbred lines selected for morphometric comparisons had different patterns of early endosperm growth (0–6 DAP) in terms of kernel-proportional endosperm area ($F_{4,\ 246}=149.79,\ P<0.0001$). Lines with small mature kernels (Hp301 and P39) had larger kernel-proportional area measures than lines with larger mature kernels (Ky21 and M162W) (P<0.05; Fig. 9). B73 was not significantly different than Hp301, but was significantly smaller than P39 and significantly larger than both Ky21 and M162W (P<0.05). Significant differences between the lines at specific DAP ($F_{24,\ 246}=5.04,\ P<0.0001$) were most apparent at 4–6 DAP, where Ky21 and M162W consistently had smaller kernel-proportional endosperm area measures than B73, Hp301, and P39 (P<0.05).

DISCUSSION

Morphometrics—B73 endosperm size during the first 12 DAP was variable, depending on the location in which it was grown. Using GDD improves the description and prediction of phenological events (McMaster and Wilhelm, 1997) by accounting for environmental differences in heat units. When GDD was used to compare endosperm lengths (either absolute or kernel-proportional) between environments (data not shown), the growth curves overlapped closely, but not as tightly as the kernel-proportional area growth curves. Given that area measurements incorporate an additional dimension of the endosperm (thickness), as well as overall endosperm shape, it was not surprising to observe more precise overlap of endosperm area growth curves than with length measurements alone. Subsequently, to account for kernel size and incorporate two dimensions of the endosperm, we chose to use kernel-proportional endosperm area measurements when examining early endosperm development among selected NAM founder lines.

Few studies report endosperm dimensions, and those that do typically give absolute endosperm length at a limited number of developmental times between 0–12 DAP (Randolph, 1936; Schel et al., 1984; Phillips and Evans, 2011). Because of the

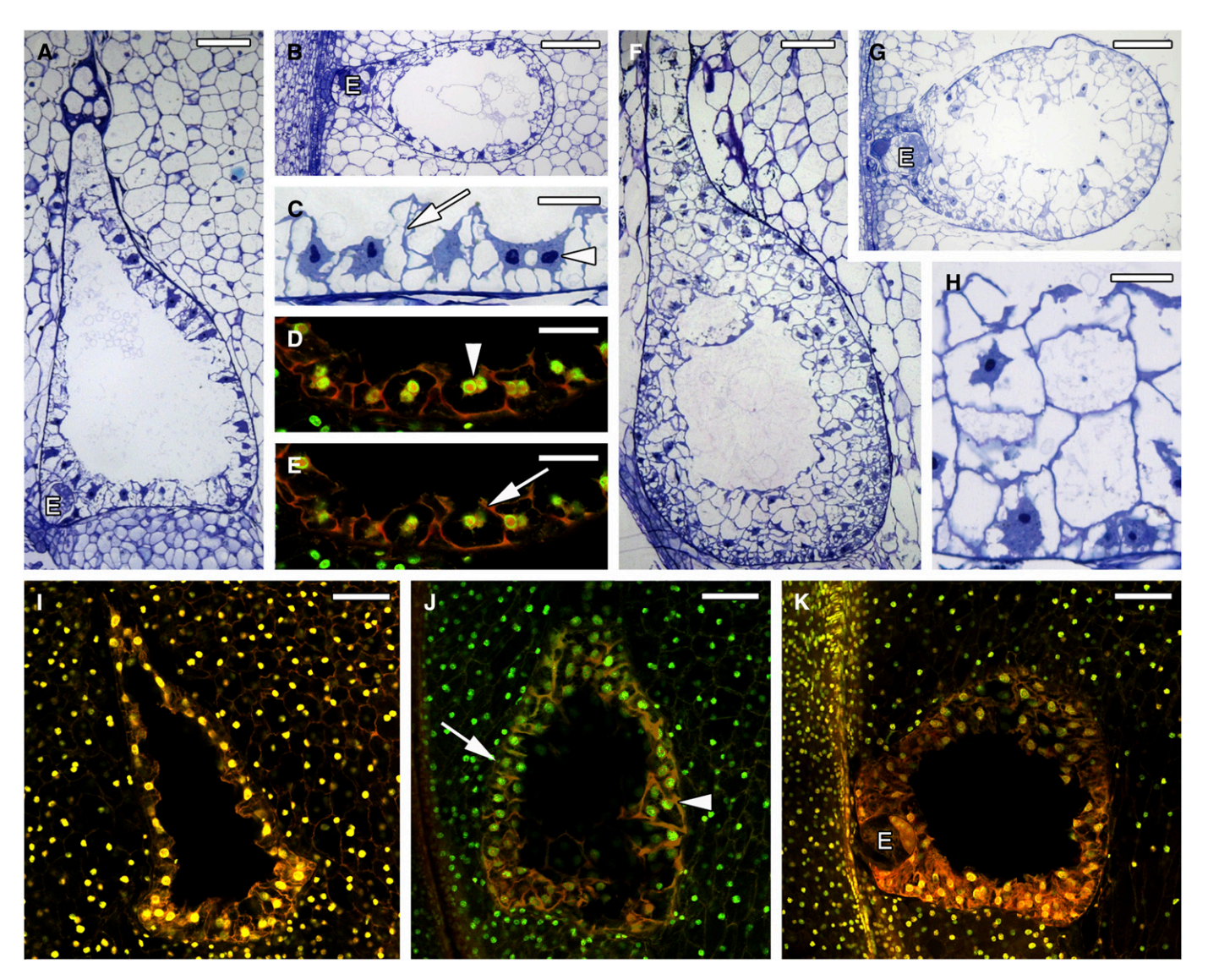
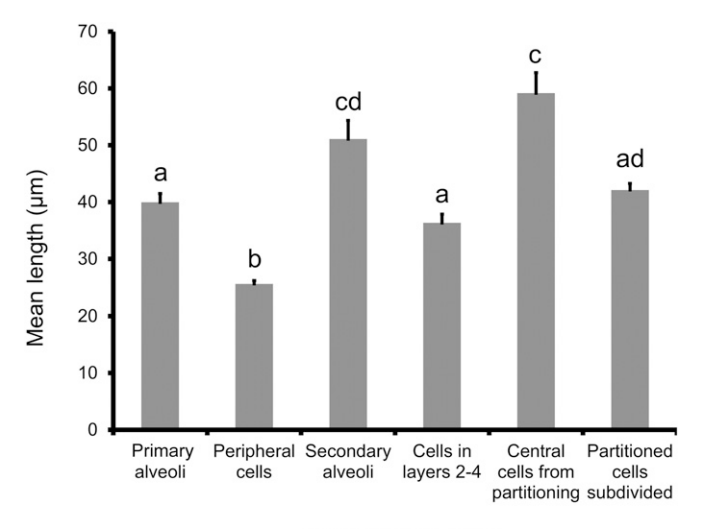


Fig. 4. Light and confocal micrographs of B73 maize endosperms during the alveolation stage of cellularization. Embryo (E) when present is to the left. Plastic sections stained with toluidine blue. For confocal microscopy, cell walls and cytoplasm (red) are stained with propidium iodide (PI) and nuclei (yellow) are double-stained with PI and SYTOX Green. (A) Longitudinal and (B) cross sections of whole endosperms showing primary alveoli. (C–E) Light and single optical confocal micrographs showing higher magnification primary alveoli with apparent anticlinal walls (arrows), with some alveoli containing two nuclei in anticlinal orientation (arrowheads). (F) Longitudinal and (G) cross sections of whole endosperms with 2–4 layers of cells formed by alveolation. Secondary alveoli are adjacent to the central vacuole. (H) High magnification of two cell files formed by alveolation. (I–K) Single optical confocal sections of three endosperms during alveolation. (I) Endosperm with alveoli complete at micropylar end and less developed toward the tip. (J) Endosperm showing nuclei in periclinal orientation before periclinal wall formation (arrow) and three nuclei in an alveolus (arrowhead). (K) Endosperm near the end of alveolation with multiple cell layers around the central vacuole. Bars = 100 μm (A, B, F, G, I–K), 50 μm (D, E), and 25 μm (C, H).

different growing conditions in these few studies (Randolph: NY field; Schel et al.: greenhouse; Phillips and Evans: both field and greenhouse), as well as line differences (Randolph: "Pride of Michigan"; Schel et al.: A-188; Phillips and Evans: W23XM14), endosperm sizes vary widely and direct comparison is difficult. In-depth growth analysis during early endosperm development allowed us to relate the cytological stages of development (coenocyte, cellularization, and differentiation) to kernel morphometrics or size.

Coenocyte—During the earliest stage of B73 endosperm development, as the triploid nucleus divides mitotically and forms a multinucleate coenocyte, endosperm size did not significantly

increase from the unfertilized embryo sac. Although we did not find any primary endosperm nucleus that divided within the first 34 h after pollination in MI material (data not shown), others have reported this to occur between 16 and 29 h after pollination (Randolph, 1936; Van Lammeren, 1981; Bedinger and Russell, 1994; Mòl et al., 1994). As the free nuclei divided, there was a progression of nuclear localization around the central vacuole from the base to the sides of the endosperm and finally throughout the periphery. The pattern of nuclear migration during formation of the initial layer of nuclei supports previous reports in maize (Randolph, 1936; Monjardino et al., 2007), but differs from *Arabidopsis*. In *Arabidopsis*, at the 16-nuclei stage, the nuclei are throughout the length of the endosperm, and



Cellularization stage

Fig. 5. B73 maize endosperm cell and alveolus length during cellularization. Standard error bars are shown; letters indicate values that differed significantly (P < 0.05). Primary alveoli are precursors to the peripheral cells. These alveoli become cells by the addition of a periclinal wall, forming a cell smaller than the alveolus from which they were formed. The secondary alveoli remaining after the peripheral cell is formed are larger than the primary alveolus. The 2–4 layers of cells formed by the secondary alveoli are larger than the peripheral cells. Subsequent central cells are formed by partitioning of the remaining central vacuole. The central cells are larger than those formed by alveolation but then undergo subdivision. All cells are smaller than the alveoli or partition from which they arose, and of the cells formed, the peripheral cells are significantly smaller than all others.

development of the central vacuole then displaces cytoplasm and nuclei to the periphery (Brown et al., 2003). We have not studied the cytoskeleton in maize, so we are unable to describe the exact mechanism of nuclear migration as has been done in barley, rice, and wheat (Brown et al., 1996b) and *Arabidopsis* (Brown et al., 1999; Boisnard-Lorig et al., 2001; Sørensen et al., 2002).

We confirmed there is synchrony of nuclear divisions in the coenocyte through nuclei counts in multiple, serially sectioned endosperms, as well as by synchronous mitotic figures within individual endosperms. Previously, Randolph (1936) and Kowles and Phillips (1988) showed coenocytic nuclei in mitosis, but not in a uniform phase of mitosis, and Kranz et al. (1998) showed synchronously dividing nuclei within the cellular endosperm of in vitro cultures. Our counts of 2ⁿ (8, 16, 64, etc.) numbers of nuclei in serially sectioned endosperms and capture of endosperms with all nuclei at the same phase of mitosis are interesting because of the tight synchrony observed. The tight synchrony of maize and other cereal endosperms is in contrast to *Arabidopsis*, where after the 16-nuclei stage, nuclear division is no longer synchronous (Boisnard-Lorig et al., 2001; Brown et al., 2003).

The number of free nuclei present at the end of the coenocytic stage in B73 is variable, with as few as 128 and as many as 512. Others have noted that free nuclear division in maize results in up to 256 (Randolph, 1936; Kiesselbach, 1949) or as many as 512 nuclei (Walbot, 1994; Sabelli and Larkins, 2009). The endosperm we observed initiating cellularization at 128 nuclei was larger than the coenocytic endosperm with 512 nuclei. Therefore, it appears that larger endosperm size may be

more coincident with initiation of cellularization rather than number of nuclei or DAP.

Cellularization—During the cellularization period of development, B73 endosperm showed its first size increase compared with the size of the prefertilization embryo sac. The initiation of cellularization was variable with regard to timing, endosperm size, and number of nuclei. Cellularization in B73 initiates ~2.5–4 DAP (~40–46 GDD) and ends at 4–5 DAP (~65–72 GDD); the process occurs rapidly, taking about 1 d. Our observations agree with those made by others for various lines of maize, with cellularization of the endosperm occurring rapidly, often being fully cellular as early as 4 DAP (Randolph, 1936; Cooper, 1951; Kowles and Phillips, 1988; Olsen, 2001). Our observations also align with a previous study of greenhouse-and field-grown W64A, where cellularization began ~43 GDD and ended ~62 GDD after pollination (Monjardino et al., 2007).

During *Arabidopsis* seed development, when the embryo is at the heart-shaped stage, the endosperm has three concurrent but different stages of endosperm development: coenocytic at the chalazal end, alveoli in the central chamber, and cellular at the micropylar end (Brown et al., 1999). In contrast, we found in maize the developmental stages occur sequentially, with the coenocytic endosperm progressing to an endosperm with alveoli throughout, which then becomes cellular endosperm. There are times when two stages intergrade, for example, the base of the endosperm having a layer of alveoli and the antipodal portion still being coenocytic, but at no time is a part of the endosperm cellular when another part is still coenocytic.

Descriptions and illustrations of the cereal endosperm cellularization process have largely been based from empirical study of developing barley and rice endosperms, as evaluation of cellularization in maize has been more limited (Randolph, 1936; Kiesselbach, 1949; Monjardino et al., 2007). Reviews and models of cereal endosperm development repeatedly describe cellularization as a repetitive two-step method of anticlinal wall growth and periclinal divisions (or alveolation) that proceeds in a centripetal manner, ultimately laying down cell files that completely close the central vacuole (e.g., Olsen, 2001, 2004; Brown and Lemmon, 2007; Sabelli and Larkins, 2009; Becraft and Gutierrez-Marcos, 2012; Olsen and Becraft, 2013). Barley endosperm becomes completely cellular after only 2-4 rounds of alveolation (Bosnes et al., 1992; Olsen and Becraft, 2013). We observed similar cell files for 2-4 rounds of alveolation, but our high-resolution images from plastic-embedded samples and confocal preparations allowed us to detect the final filling of the central vacuole in maize occurs by a random, less precise cell formation process we describe as partitioning. Our model provides a more accurate account of maize endosperm cellularization than current cereal endosperm models that are based largely on the smaller grain species.

Throughout cellularization, we expected each alveolus to contain a single nucleus, or two nuclei in a periclinal plane if mitosis had just occurred. Olsen (2001) noted orientation of nuclear division during cellularization is in the periclinal plane and speculated that this is partially due to space constraints of the small barley kernel. Rather, during alveolation, we observed some alveoli with two nuclei oriented in an anticlinal plane. Likewise, during alveolation and partitioning, we observed three or more nuclei in some alveoli. Monjardino et al. (2007) described nuclei with periclinal and anticlinal orientations, and they presumed the anticlinal orientation reflected recent nuclear

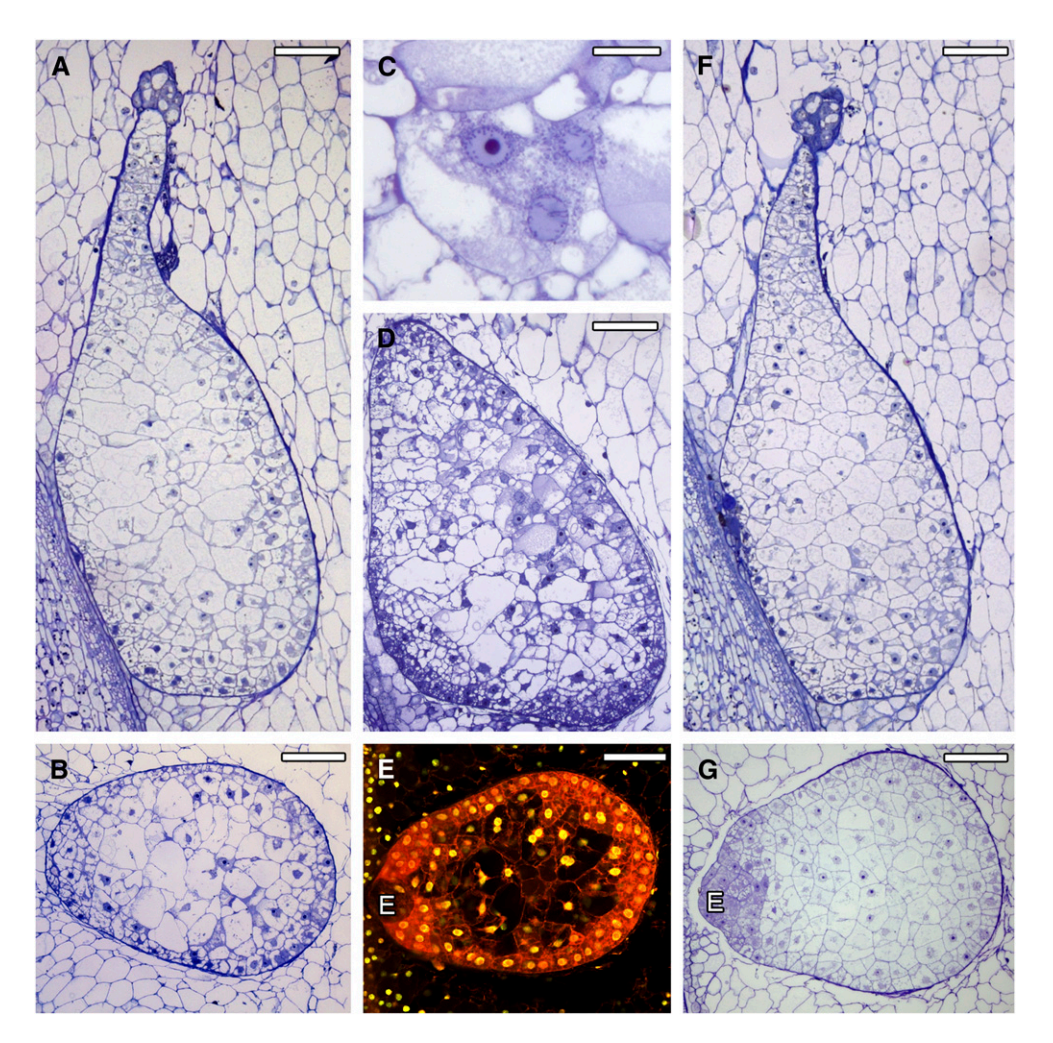


Fig. 6. Light and confocal micrographs of B73 maize endosperms during the partitioning stage of cellularization. Embryo (E) when present is to the left. Plastic sections stained with toluidine blue. For confocal microscopy, cell walls and cytoplasm (red) are stained with propidium iodide (PI) and nuclei (yellow) are double-stained with PI and SYTOX Green. (A) Longitudinal and (B) cross sections of whole endosperms showing anticlinal cell walls extend until the central vacuole is completely partitioned. (C–E) Light and single optical section micrographs with large compartments further subdividing into smaller cells, some with up to three nuclei (C), in an unorganized fashion. (F) Longitudinal and (G) cross sections of whole endosperms with subdivided central cells and fully cellular endosperms. Bars = $100 \, \mu m$ (A, B, D–G) and $25 \, \mu m$ (C).

divisions. However, that does not explain three or more nuclei in an alveolus, as we have observed, and we note can be seen in the image of Monjardino et al. (2007: see fig. 2B). We suspect anticlinal cell wall formation is not uniform in the large maize kernel. Primary anticlinal walls form earlier and faster than periclinal nuclear division and wall formation. The different rate at which the walls form accounts for the large compartments observed at the end of cellularization. The rapidly extending anticlinal walls compartmentalize the entire endosperm (for example, Fig. 6A) before lagging nuclear divisions and periclinal walls can form new cells. Once the central vacuole is partitioned, nuclei divide and cells form in a less organized fashion than occurs at the periphery. Monjardino et al. (2007) observed maize endosperm cellularization (also using kernels embedded in plastic resin) and described unorganized alveoli that rapidly formed cells in the central vacuole during late cellularization, which corresponds with our description of partitioning. The large, irregular cells formed during partitioning may help explain how the large and uniquely shaped maize

endosperm so quickly cellularizes. Partitioning could also explain the absence of distinct cell files in the central region.

Differentiation—Differentiation of the cellular B73 endosperm into aleurone, subaleurone, SE, BETL, ESR, CZ, and our newly identified BIZ occurs over approximately 6 d of development. Soon after cellularization is complete, ESR, SE, aleurone, and BETL cell types become distinguishable by structure and location; in later differentiation, these cell types are further distinguished and the subaleurone, BIZ and CZ are evident. The following descriptions, based on our observations in B73, largely reiterate previous reports with other maize lines for: ESR (Kiesselbach and Walker, 1952; Schel et al., 1984; Opsahl-Ferstad et al., 1997), aleurone and subaleurone (Weatherwax, 1930; Kyle and Styles, 1977), and SE (Weatherwax, 1930; Lampe, 1931; Monjardino et al., 2007). Cells constituting the ESR are small, isodiametric, cytoplasm-dense cells adjacent to the embryo that differentiate early, and later appear to be crushed by the growing embryo and are distinct only near the

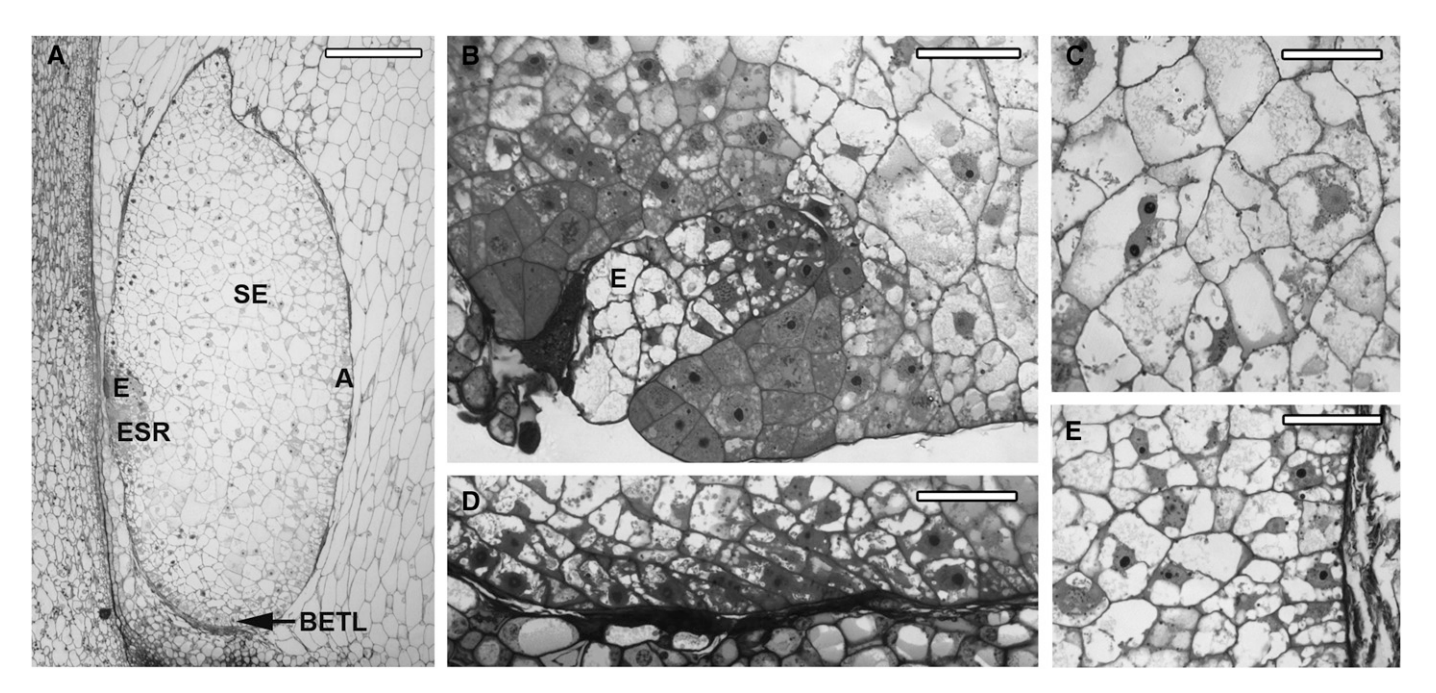


Fig. 7. Light micrographs of B73 maize endosperms during early differentiation. Plastic sections stained with toluidine blue. (A) Longitudinal section through a whole endosperm showing four distinguishable cell types in early differentiation. (B) ESR of densely cytoplasmic cells most prominent around the suspensor portion of embryo. (C) Large SE cells before starch deposition. (D) BETL showing beginning of elongated cells but before wall ingrowths are apparent. (E) Aleurone cells developing multiple large conspicuous vacuoles. *Abbreviations*: A, aleurone; BETL, basal endosperm transfer layer; E, embryo; ESR, embryo surrounding region; SE, starchy endosperm. Bars = 200 μm (A) and 50 μm (B–E).

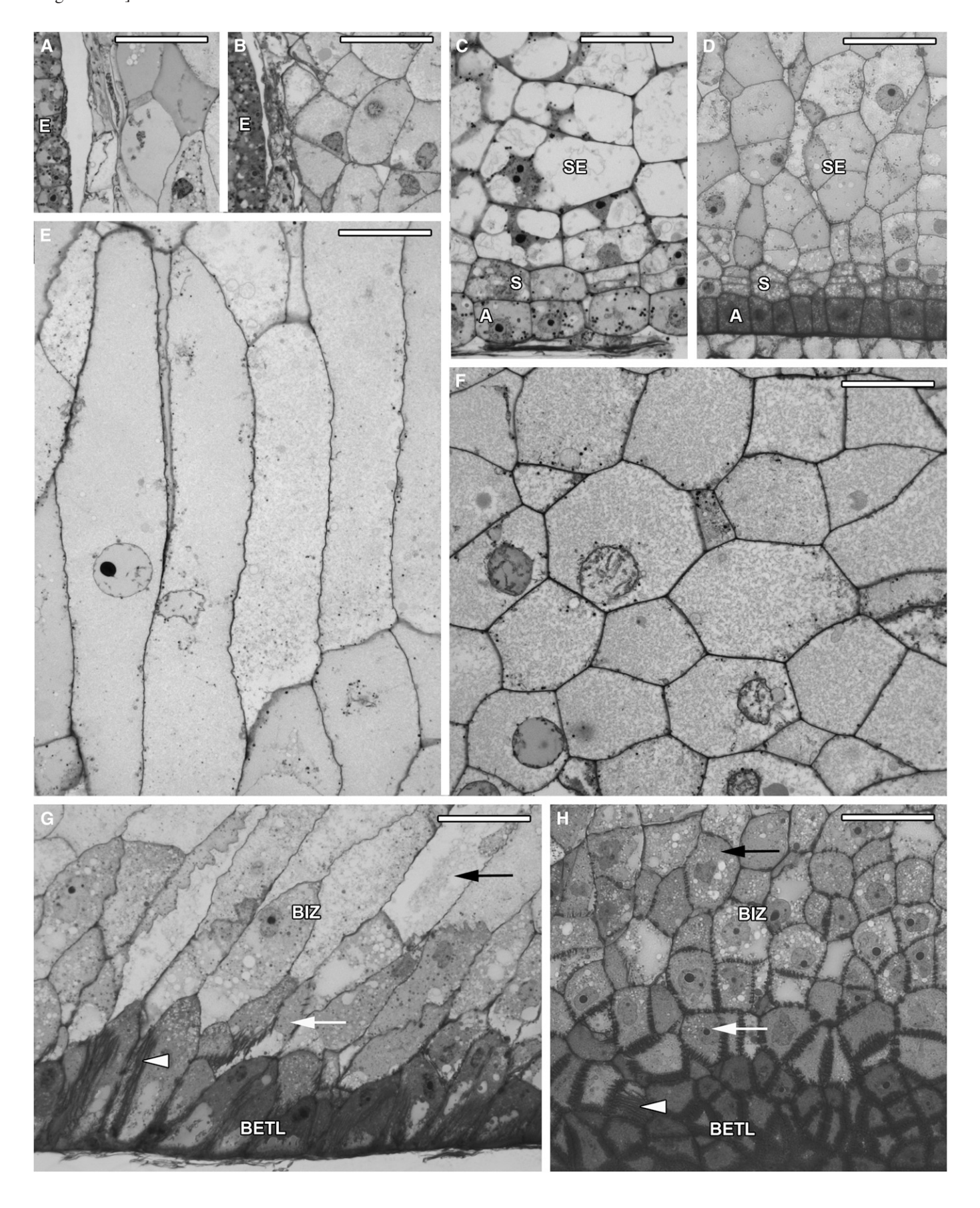
suspensor region. Aleurone cells are distinguishable at the end of cellularization and continue to maintain their boxy shape as they develop a dense cytoplasm with a few small vacuoles and accumulate lipids later in differentiation. Though subaleurone cells are not pointedly different in size and shape than aleurone cells, their meristematic activity later in differentiation is fundamental to their identification. Large immature SE cells are apparent early in the central portion of the endosperm, and their shape and size become irregular later in differentiation.

In the lower portion of the endosperm are three elongated cell types: BETL, BIZ, and CZ. In addition to cytological differences among them, their long-axis lengths are significantly different. Cells comprising the BIZ have often been grouped with either the BETL or CZ as a cell type (e.g., Becraft, 2001), and sometimes authors simply refer to transfer cells and fail to identify CZ specifically (e.g., Olsen, 2001). We determined cells in the BIZ do not have characteristics identical with either of the adjacent cell types and therefore warranted a distinct name. We specified this area as the BIZ (basal intermediate zone), because cells in this region are intermediate in both location and cellular characteristics compared to the adjacent BETL and CZ.

In maize, cells that exhibit transfer cell morphology include the single basal layer directly above the chalazal pad, and the adjacent 3-4 cell layers that contain a gradient of ingrowths decreasing toward the interior of the endosperm (Kiesselbach and Walker, 1952; Schel et al., 1984; Davis et al., 1990; Gao et al., 1998; Thompson et al., 2001; Monjardino et al., 2013). Most authors identify the single layer of transfer cells directly above the chalazal pad as being morphologically distinct, often referred to as the BETL. The BETL is characterized by relatively large, elongate cells with extensive wall ingrowths, which are thought to aid in metabolite transfer through an increase of the plasma membrane surface area (Kiesselbach and Walker, 1952; Becraft, 2001). We defined the BETL as the most basal layer of cells in this region with the most pronounced characteristics, and the adjacent area displaying a gradient of less numerous cell wall ingrowths as the BIZ.

The most basal single cell layer (BETL) and the layer 2–4 cells thick immediately above (BIZ) have been differentiated based on their respective cellular morphologies. Monjardino et al. (2013) termed the initial transfer cell layer "most basal endosperm transfer cells" due to the distinguishing cell wall ingrowth morphologies between this layer (BETL) and the

Fig. 8. Light micrographs of longitudinal and cross sections of B73 maize endosperm showing seven distinguishable cell types later in differentiation. Plastic sections stained with toluidine blue. For each cell type, the left image is a longitudinal section and the right image is a cross section. (A, B) ESR of densely cytoplasmic cells most prominent around the suspensor portion of the embryo. (C, D) Endosperm edge showing aleurone and SE cells along with characteristic meristematic area of the subaleurone that leads to production of more SE cells. (E, F) Conducting zone of very elongate cells with large nuclei. (G, H) BETL cells showing dense cytoplasm and heavy wall ingrowths (arrowheads). BIZ cells showing intermediate characteristics. BIZ cells adjacent to BETL show small wall ingrowths and dense cytoplasm (white arrows). BIZ cells nearer CZ (black arrows) are longer with less-dense cytoplasm. *Abbreviations:* A, aleurone; BETL, basal endosperm transfer layer; BIZ, basal intermediate zone; CZ, conducting zone; E, embryo; ESR, embryo surrounding region; S, subaleurone; SE, starchy endosperm. Scale bars = 50 μm.



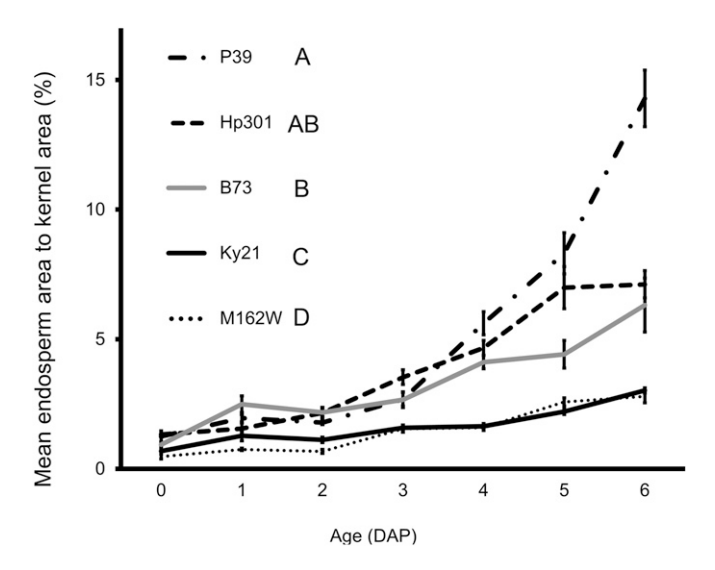


Fig. 9. Comparison of endosperm growth in B73 and four NAM founder lines over the first 6 d after pollination (DAP). Bars indicate standard errors. Letters next to legend indicate differences among the lines (P < 0.05).

adjacent cells (our BIZ). The cell wall ingrowths observed in the BETL are both reticulate and flange, whereas the cells comprising the BIZ only contain flange ingrowths (Monjardino et al., 2013). Additionally, RNA transcripts (BETL-1, -2, -3, -4) and their respective proteins (Hueros et al., 1995, 1999), have been localized that transverse both the BETL and BIZ, and are coincident with the spatiotemporal onset of cell wall ingrowths. Other unique RNA transcripts (MRP-1; Gómez et al., 2002, 2009) are restricted to only the most basal cells (our BETL) and have been shown to induce transfer cell-like fate when ectopically expressed in the aleurone layer. More recent work has identified unique BETL- and BIZ-specific transcripts (Li et al., 2014). Differential gene expression and the presence of different types of cell wall ingrowths in these two regions, along with our observations and cell measurements, support separation of the BETL and BIZ into two distinct zones.

We observed a subset of cells within the endosperm that are extremely elongated with extremely large nuclei. This column of elongated cells extends from BIZ toward the central portion of the endosperm. This region, an area of elongated cells presumably providing a primitive vascular function (Weatherwax, 1930; Lampe, 1931) has been described as the conducting zone (Brink and Cooper, 1947; Cooper, 1951; Becraft, 2001). Cells in the CZ appear to have less dense cytoplasm than the adjacent BIZ and SE, and are easily identifiable as a morphologically unique region. Additionally, recent gene expression analysis identified specific transcripts that were detected within CZ, BIZ, and SE cells (Li et al., 2014). The CZ has previously been identified as a distinct region based on cellular characteristics; our cytological observations and cell measurements, along with differential gene expression, justify its separation from the adjacent BIZ and SE.

NAM founder endosperm growth patterns—Our analysis of select NAM founder inbred lines revealed that mature kernel size may be a predictor of early endosperm growth. Inbreds with larger mature kernel size (non-stiff stalk lines Ky21 and M162W) had slower endosperm growth through 6 DAP compared

to inbreds with smaller mature kernel size (sweet corn line P39 and popcorn line Hp301). Kernel-proportional length and thickness showed a similar pattern to area (data not shown).

Jones et al. (1996) studied (from 10-32 DAP) the mass of small and large kernel maize inbreds that were further classified as early or late maturing lines. Kernel mass of A619 (large, early maturing) was greater than that of W64A (small, early maturing) during late portions of the lag phase (10–18 DAP; preceding the linear grain filling phase), though both early maturity inbreds had greater kernel mass than Mo17 (large, late maturing) and B73 (small, late maturing) during the same period (Jones et al., 1996). In contrast, kernel growth rate in large kernel inbreds (regardless of maturity) was nearly 2-fold higher than that of small kernel inbreds during the grain-filling period (20-32 DAP), resulting in greater kernel mass of large kernel inbreds during most of this period and at maturity (Jones et al., 1996). These observations support those made earlier by Reddy and Daynard (1983) that maize endosperm cell number, starch granule number, rate of grain filling, and kernel mass at maturity are all positively correlated. Cross (1975) observed that maize hybrids with long lag phases tended to have faster rates of grain filling. Likewise, Bagnara and Daynard (1982) found positive associations between length of the lag phase, overall rate of endosperm growth, and maximum endosperm dry mass. These observations, among others, have led to the suggestion that events during the lag period influence storage capacity of the endosperm by establishing the number of cells per endosperm and starch granules per cell. However, since grain dry matter accumulation is negligible during the lag period (reviewed in Severini et al., 2011), these studies of endosperm and kernel mass did not include the earliest and most formative portions of the endosperm lag phase.

Our work with B73 showed that patterns of endosperm size during the earliest portion of the lag phase (1–12 DAP) appeared to directly correlate with timing of cytological events. Our preliminary NAM analysis suggests that lines with small mature kernels have larger endosperms earlier in development, which may indicate small kernel lines complete important cytological events at a faster rate than large kernel lines. This hypothesis aligns with observations of earlier onset and more rapid termination of endoreduplication in popcorn (small kernel) lines when compared with large kernel dent inbreds (Dilkes et al., 2002). The measurements presented here allow us to now study and compare maize endosperm development across diverse lines as a way to evaluate patterns of early growth and identify potential differences in timing of cellularization.

Conclusions: Impacts of large kernel size on maize endosperm development—Many of our descriptions of maize endosperm development could be a consequence of its large size compared with other cereals and Arabidopsis. We observed that initiation of maize endosperm cellularization may be more coincident with size than the number of nuclei or their age, as suggested by previous authors (e.g., Randolph, 1936; Kiesselbach, 1949; Walbot, 1994). The plane of nuclear division in alveoli may be constrained by endosperm size. Nuclear divisions within alveoli of barley are only in periclinal planes, which Olsen (2001) suggested may be due to space constraints; however, the anticlinal divisions we observed suggest the large size of maize endosperm may allow more diverse planes of cell division. Moreover, we observed the larger maize endosperm size requires partitioning to complete cellularization, a process in addition to alveolation. This contrasts with barley, rice, wheat, and *Arabidopsis*, which only cellularize through repeated alveolation (Brown et al., 1999; Olsen, 2001, 2004; Brown and Lemmon, 2007).

Though there is diversity across the cereals and *Arabidopsis* in the number and complexity of differentiated cell types, all have a portion of the endosperm dedicated to aleurone and transfer-celllike functions. For example, possible nutrient transport systems in the endosperm can range from coenocytic cysts (*Arabidopsis*) or one layer of specialized basal cells (barley) (Olsen and Becraft, 2013), to three specialized basal cell types (maize) (this study); these observations suggest that with increasing endosperm size there is an increased number and complexity of cell types required for shuttling of nutrients from maternal tissues to the developing endosperm and embryo. Further, we show that cell size is important for distinguishing the BETL, BIZ, and CZ cell types within maize. Lastly, early endosperm development may also impact kernel size across diverse lines of maize. Comparison of diverse NAM lines suggests differences in mature kernel size may be conditioned during early development, with small kernel lines having larger endosperms during early development. Continued studies of the NAM lines will provide information relevant to how early endosperm size may influence timing of cytological development and mature kernel size.

LITERATURE CITED

- BAGNARA, D., AND T. B. DAYNARD. 1982. Rate and duration of kernel growth in the determination of maize (*Zea mays* L.) kernel size. *Canadian Journal of Plant Science* 62: 579–587.
- Becraft, P. W. 2001. Cell fate specification in the cereal endosperm. Seminars in Cell & Developmental Biology 12: 387–394.
- Becraft, P. W., and J. Gutierrez-Marcos. 2012. Endosperm development: Dynamic processes and cellular innovations underlying sibling altruism. *WIREs Developmental Biology* 1: 579–593.
- Bedinger, P., and S. D. Russell. 1994. Gametogenesis in maize. *In M.* Freeling and V. Walbot [eds.], The maize handbook, 48–61. Springer-Verlag, New York, New York, USA.
- Bennett, M. D., J. B. Smith, and I. Barclay. 1975. Early seed development in the Triticeae. *Philosophical Transactions of the Royal Society of London, B, Biological Sciences* 272: 199–227.
- Boisnard-Lorig, C., A. Colon-Carmona, M. Bauch, S. Hodge, P. Doerner, E. Bancharel, C. Dumas, et al. 2001. Dynamic analyses of the expression of the HISTONE:YFP fusion protein in *Arabidopsis* show that syncytial endosperm is divided in mitotic domains. *Plant Cell* 13: 495–509.
- Bosnes, M., F. Weideman, and O.-A. Olsen. 1992. Endosperm differentiation in barley wild-type and sex mutants. *Plant Journal* 2: 661–674.
- Brink, R. A., and D. C. Cooper. 1947. Effect of the De₁₇ allele of development of the maize caryopsis. *Genetics* 32: 350–368.
- Brown, R. C., and B. E. Lemmon. 2007. The developmental biology of cereal endosperm. *Plant Cell Monographs* 8: 1–20.
- Brown, R. C., B. E. Lemmon, and H. Nguyen. 2003. Events during the first four rounds of mitosis establish three developmental domains in the syncytial endosperm of *Arabidopsis thaliana*. *Protoplasma* 222: 167–174.
- Brown, R. C., B. E. Lemmon, H. Nguyen, and O.-A. Olsen. 1999. Development of endosperm in *Arabidopsis thaliana*. *Sexual Plant Reproduction* 12: 32–42.
- Brown, R. C., B. E. Lemmon, and O.-A. Olsen. 1994. Endosperm development in barley: Microtubule involvement in the morphogenetic pathway. *Plant Cell* 6: 1241–1252.
- Brown, R. C., B. E. Lemmon, and O.-A. Olsen. 1996a. Development of the endosperm in rice (*Oryza sativa* L.): Cellularization. *Journal of Plant Research* 109: 301–313.
- Brown, R. C., B. E. Lemmon, and O.-A. Olsen. 1996b. Polarization predicts the pattern of cellularization in cereal endosperm. *Protoplasma* 192: 168–177.

- Brown, R. C., B. E. Lemmon, B. A. Stone, and O.-A. Olsen. 1997. Cell wall $(1 \rightarrow 3)$ and $(1 \rightarrow 3, 1 \rightarrow 4)$ -β-glucans during early grain development in rice (*Oryza sativa* L.). *Planta* 202: 414–426.
- Buckler, E. S., B. S. Gaut, and M. D. McMullen. 2006. Molecular and functional diversity of maize. *Current Opinion in Plant Biology* 9: 172–176.
- COOPER, D. C. 1951. Caryopsis development following matings between diploid and tetraploid strains of *Zea mays. American Journal of Botany* 38: 702–708.
- Costa, L. M., J. F. Gutierrez-Marcos, T. P. Brutnell, A. J. Greenland, and H. G. Dickinson. 2003. The *globby1-1* (*glo1-1*) mutation disrupts nuclear and cell division in the developing maize seed causing alterations in endosperm cell fate and tissue differentiation. *Development* 130: 5009–5017.
- CROSS, H. Z. 1975. Diallel analysis of duration and rate of grain filling of seven inbred lines of corn. *Crop Science* 15: 532–535.
- CROSS, H. Z., AND M. S. ZUBER. 1972. Prediction of flowering dates in maize based on different methods of estimating thermal units. *Agronomy Journal* 64: 351–355.
- DAVIS, R. W., J. D. SMITH, AND B. G. COBB. 1990. A light and electron microscope investigation of the transfer cell region of maize caryopses. *Canadian Journal of Botany* 68: 471–479.
- DILKES, B. P., R. A. DANTE, C. COELHO, AND B. A. LARKINS. 2002. Genetic analyses of endoreduplication in *Zea mays* endosperm: Evidence of sporophytic and zygotic maternal control. *Genetics* 160: 1163–1177.
- DOAN, D. N. P., C. LINNESTAD, AND O.-A. OLSEN. 1996. Isolation of molecular markers from the barley endosperm coenocyte and the surrounding nucellus cell layers. *Plant Molecular Biology* 31: 877–886.
- DREA, S., D. J. LEADER, B. C. ARNOLD, P. SHAW, L. DOLAN, AND J. H. DOONAN. 2005. Systematic spatial analysis of gene expression during wheat caryopsis development. *Plant Cell* 17: 2172–2185.
- FINERAN, B. A., D. J. C. WILD, AND M. INGERFELD. 1982. Initial wall formation in the endosperm of wheat, *Triticum aestivum*: A reevaluation. *Canadian Journal of Botany* 60: 1776–1795.
- FLINT-GARCIA, S. A., A.-C. THUILLET, J. YU, G. PRESSOIR, S. M. ROMERO, S. E. MITCHELL, J. DOEBLEY, ET AL. 2005. Maize association population: A high-resolution platform for quantitative trait loci dissection. *Plant Journal* 44: 1054–1064.
- FLOYD, S. K., AND W. E. FRIEDMAN. 2000. Evolution of endosperm developmental patterns among basal flowering plants. *International Journal of Plant Sciences* 161: S57–S81.
- GAO, R., S. DONG, J. FAN, AND C. Hu. 1998. Relationship between development of endosperm transfer cells and grain mass in maize. *Biologia Plantarum* 41: 539–546.
- GÓMEZ, E., J. ROYO, Y. GUO, R. THOMPSON, AND G. HUEROS. 2002. Establishment of cereal endosperm expression domains: Identification and properties of a maize transfer cell-specific transcription factor, ZmMRP-1. Plant Cell 14: 599–610.
- Gómez, E., J. Royo, L. M. Muniz, O. Sellam, W. Paul, D. Gerentes, C. Barrero, et al. 2009. The maize transcription factor Myb-Related Protein-1 is a key regulator of the differentiation of transfer cells. *Plant Cell* 21: 2022–2035.
- GUTIERREZ-MARCOS, J. F., L. M. COSTA, AND M. M. S. EVANS. 2006. Maternal gametophyte baseless 1 is required for development of the central cell and early endosperm patterning in maize (*Zea mays*). *Genetics* 174: 317–329.
- HUEROS, G., J. ROYO, M. MAITZ, F. SALAMINI, AND R. D. THOMPSON. 1999. Evidence for factors regulating transfer cell-specific expression in maize endosperm. *Plant Molecular Biology* 41: 403–414.
- HUEROS, G., S. VAROTTO, F. SALAMINI, AND R. D. THOMPSON. 1995. Molecular characterization of *BETI*, a gene expressed in the endosperm transfer cells of maize. *Plant Cell* 7: 747–757.
- JONES, R. J., B. M. N. SCHREIBER, AND J. A. ROESSLER. 1996. Kernel sink capacity in maize: Genotypic and maternal regulation. *Crop Science* 36: 301–306.
- KIESSELBACH, T. A. 1949. The structure and reproduction of corn. University of Nebraska Agricultural Experiment Station Research Bulletin 161: 1–96.

- KIESSELBACH, T. A., AND E. R. WALKER. 1952. Structure of certain specialized tissues in the kernel of corn. American Journal of Botany 39: 561–569.
- Kowles, R. V., and R. L. Phillips. 1988. Endosperm development in maize. *International Review of Cytology* 112: 97–136.
- Kranz, E., P. von Wiegen, H. Quader, and H. Lörz. 1998. Endosperm development after fusion of isolated, single maize sperm and central cells in vitro. *Plant Cell* 10: 511–524.
- Kyle, D. J., and E. D. Styles. 1977. Development of aleurone and subaleurone layers in maize. *Planta* 137: 185–193.
- LAMPE, L. 1931. A microchemical and morphological study of the developing endosperm of maize. *Botanical Gazette* 91: 337–376.
- LI, G., D. WANG, R. YANG, K. LOGAN, H. CHEN, S. ZHANG, M. I. SKAGGS, ET AL. 2014. Temporal patterns of gene expression in developing maize endosperm identified through transcriptome sequencing. *Proceedings* of the National Academy of Sciences, USA 111: 7582–7587.
- LIU, K. J., M. GOODMAN, S. MUSE, J. S. SMITH, E. BUCKLER, AND J. DOEBLEY. 2003. Genetic structure and diversity among maize inbred lines as inferred from DNA microsatellites. *Genetics* 165: 2117–2128.
- Mansfield, S. G., and L. B. Briarty. 1990. Endosperm cellularization in *Arabidopsis thaliana* L. *Arabidopsis Electronic Information Service* 27: 65–72.
- Mares, D. J., K. Norstog, and B. A. Stone. 1975. Early stages in the development of wheat endosperm. I. The change from free nuclear to cellular endosperm. *Australian Journal of Botany* 23: 311–326.
- MARES, D. J., B. A. STONE, C. JEFFERY, AND K. NORSTOG. 1977. Early stages in the development of wheat endosperm. II. Ultrastructural observation on cell wall formation. *Australian Journal of Botany* 25: 599–613.
- McMaster, G. S., and W. W. Wilhelm. 1997. Growing degree-days: One equation, two interpretations. *Agricultural and Forest Meteorology* 87: 291–300.
- McMullen, M. D., S. Kresovich, H. S. Villeda, P. Bradbury, H. H. Li, Q. Sun, S. Flint-Garcia, et al. 2009. Genetic properties of the maize nested association mapping population. *Science* 325: 737–740.
- Mòl, R., E. Matthys-Rochon, and C. Dumas. 1994. The kinetics of cytological events during double fertilization in *Zea mays* L. *Plant Journal* 5: 197–206.
- MONJARDINO, P., J. MACHADO, F. S. GIL, R. FERNANDES, AND R. SALEMA. 2007. Structural and ultrastructural characterization of maize coenocyte and endosperm cellularization. *Canadian Journal of Botany* 85: 216–223.
- MONJARDINO, P., S. ROCHA, A. C. TAVARES, R. FERNANDES, P. SAMPAIO, R. SALEMA, AND A. D. MACHADO. 2013. Development of flange and reticulate wall ingrowths in maize (*Zea mays* L.) endosperm transfer cells. *Protoplasma* 250: 495–503.
- MORRISON, I. N., AND T. P. O'BRIEN. 1976. Cytokinesis in the developing wheat grain; division with and without a phragmoplast. *Planta* 130: 57–67.
- Olsen, O.-A. 2001. Endosperm development: Cellularization and cell fate specification. *Annual Review of Plant Physiology and Plant Molecular Biology* 52: 233–267.
- OLSEN, O.-A. 2004. Nuclear endosperm development in cereals and Arabidopsis thaliana. Plant Cell 16: S214–S227.
- OLSEN, O.-A., AND P. W. BECRAFT. 2013. Endosperm development. In P. W. Becraft [ed.], Seed genomics, 43–62. Wiley-Blackwell, Hoboken, New Jersey, USA.
- Olsen, O.-A., R. C. Brown, and B. E. Lemmon. 1995. Pattern and process of wall formation in developing endosperm. *BioEssays* 17: 803–812.

- Olsen, O.-A., C. Linnestad, and S. E. Nichols. 1999. Developmental biology of the cereal endosperm. *Trends in Plant Science* 4: 253–257.
- Opsahl-Ferstad, H. G., E. Le Deunff, C. Dumas, and P. M. Rogowsky. 1997. *ZmEsr*, a novel endosperm-specific gene expressed in a restricted region around the maize embryo. *Plant Journal* 12: 235–246.
- PHILLIPS, A. R., AND M. M. S. EVANS. 2011. Analysis of *stunter1*, a maize mutant with reduced gametophyte size and maternal effects on seed development. *Genetics* 187: 1085–1097.
- Randolph, L. F. 1936. Developmental morphology of the caryopsis in maize. *Journal of Agricultural Research* 53: 881–916.
- REDDY, V. M., AND T. B. DAYNARD. 1983. Endosperm characteristics associated with rate of grain filling and kernel size in corn. *Maydica* 28: 339–355.
- Ruzin, S. E. 1999. Plant microtechnique and microscopy. Oxford University Press, New York, New York, USA.
- SABELLI, P. A., AND B. A. LARKINS. 2009. The development of endosperm in grasses. *Plant Physiology* 149: 14–26.
- SCHEL, J. H. N., H. KIEFT, AND A. A. M. VAN LAMMEREN. 1984. Interactions between embryo and endosperm during early developmental stages of maize caryopses (*Zea mays*). *Canadian Journal of Botany* 62: 2842–2853
- Schnable, P. S., D. Ware, R. S. Fulton, J. C. Stein, F. S. Wei, S. Pasternak, C. Z. Liang, et al. 2009. The B73 maize genome: Complexity, diversity, and dynamics. *Science* 326: 1112–1115.
- SEVERINI, A. D., L. BORRÁS, M. E. WESTGATE, AND A. G. CIRILO. 2011. Kernel number and kernel weight determination in dent and popcorn maize. *Field Crops Research* 120: 360–369.
- SØRENSEN, M. B., U. MAYER, W. LUKOWITZ, H. ROBERT, P. CHAMBRIER, G. JÜRGENS, C. SOMERVILLE, ET AL. 2002. Cellularisation in the endosperm of *Arabidopsis thaliana* is coupled to mitosis and shares multiple components with cytokinesis. *Development* 129: 5567–5576.
- SPRINGER, N. M., K. YING, Y. Fu, T. JI, C.-T. YEH, Y. JIA, W. WU, ET AL. 2009. Maize inbreds exhibit high levels of copy number variation (CNV) and presence/absence variation (PAV) in genome content. PLOS Genetics 5: e1000734.
- Spurr, A. R. 1969. A low-viscosity epoxy resin embedding medium for electron microscopy. *Journal of Ultrastructure Research* 26: 31–43.
- Strable, J., and M. J. Scanlon. 2009. Maize (*Zea mays*): A model organism for basic and applied research in plant biology. *Cold Spring Harbor Protocols* 4: 1–9.
- Thompson, R. D., G. Hueros, H. A. Becker, and M. Maitz. 2001. Development and functions of seed transfer cells. *Plant Science* 160: 775–783.
- Van Lammeren, A. A. M. 1981. Early events during embryogenesis in *Zea mays* L. *Acta Societatis Botanicorum Poloniae* 50: 289–290.
- Van Lammeren, A. A. M. 1988. Structure and function of the microtubular cytoskeleton during endosperm development in wheat: An immunofluorescence study. *Protoplasma* 146: 18–27.
- WALBOT, V. 1994. Overview of key steps in aleurone development. In M. Freeling and V. Walbot [eds.], The maize handbook, 78–80. Springer-Verlag, New York, New York, USA.
- Weatherwax, P. 1930. The endosperm of *Zea* and *Coix. American Journal of Botany* 17: 371–380.
- WILLIAMS, J. H., AND W. E. FRIEDMAN. 2002. Identification of diploid endosperm in an early angiosperm lineage. *Nature* 415: 522–526.
- Yu, J., J. B. Holland, M. D. McMullen, and E. S. Buckler. 2008. Genetic design and statistical power of nested association mapping in maize. *Genetics* 178: 539–551.